

DeepProg: A Multi-modal Transformer-based End-to-end Framework for Predicting Disease Prognosis

Huy Hoang Nguyen¹, Simo Saarakkala^{1,2},
Matthew B. Blaschko³, and Aleksei Tiulpin^{1,4,5}

¹ Research Unit of Medical Imaging, Physics and Technology,
University of Oulu, Finland

² Department of Diagnostic Radiology, Oulu University Hospital, Finland

³ Center for Processing Speech & Images, KU Leuven, Belgium

⁴ Aalto University, Finland

⁵ Ailean Technologies Oy, Finland

huy.nguyen@oulu.fi

Abstract. A vast majority of deep learning methods are built to automate diagnostic tasks. However, in clinical practice, a more advanced question is how to predict the course of a disease. Current methods for this problem are complicated, and often require domain knowledge, making them difficult for practitioners to use. In this paper, we formulate the prognosis prediction task as a one-to-many sequence prediction problem. Inspired by a clinical decision making process with two agents – a radiologist and a general practitioner – we propose a generic end-to-end transformer-based framework to estimate disease prognosis from images and auxiliary data. The effectiveness and validation of the developed method are shown on synthetic data, and in the task of predicting the development of structural osteoarthritic changes in knee joints.

1 Introduction

Osteoarthritis (OA) is the most common musculoskeletal disorder that affects millions of people around the world [1]. Among all the joints in the body, OA is mostly prevalent in knee [2]. Knee OA (further – OA) is characterized by the breakdown of knee joint cartilage, the appearance of osteophytes, and the narrowing of joint space [2], which are imaged using X-ray (radiography). The disease severity is graded according to the Kellgren-Lawrence system [3] from 0 (no OA) to 4 (end stage OA). We illustrate this grading in Suppl. Figure S1. An example of a knee progressing according to this system and imaged by radiography is illustrated in Figure 1.

Unfortunately, no cure has yet been developed for OA. However, the detection of the disease, and prediction of its course at early stages, may enable treatment to slow down its development. Recent works in the field of OA focused on detecting it from images [4,5], and other studies worked on predicting *whether* OA will progress [6,7,8] (progression prediction problem). To the best of our knowledge, there are no studies on the subject of OA that tackle the issue

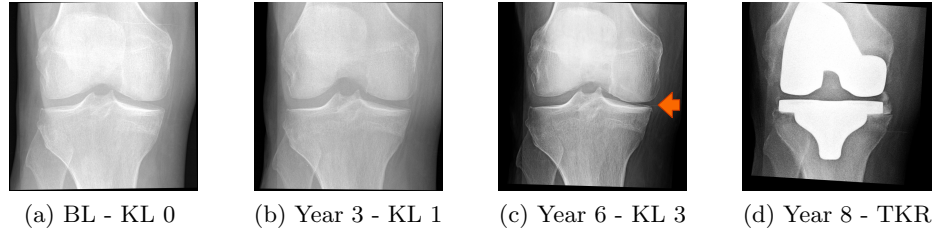


Fig. 1. Radiographs of a patient with OA progressed in 8 years. Red arrow indicates joint space narrowing. The disease progressed from Kellgren-Lawrence (KL) grade 0 at the baseline (BL) to 3 in 6 years. At the 8th year, the patient underwent a total knee replacement (TKR) surgery.

of predicting *how* the disease will evolve in time (prognosis prediction problem). In this study, we tackle this problem, and our contributions are the following:

1. We propose a novel transformer-based multi-modal framework that allows to predict the development of a disease from multi-modal data available at a single examination.
2. An application of our method is shown on synthetic data, based on the Chest MNIST dataset [9], as well as on real OA progression data. To the best of our knowledge, this is the first study on predicting a fine-grained prognosis of knee OA from raw image data.
3. We show that our method also performs fine-grained progression predictions alongside the prognosis prediction task, and outperforms the state-of-the-art (SOTA).

2 Related Work

Knee osteoarthritis The attention of the literature has gradually been shifting from diagnosing the current OA severity of a knee to predicting whether degenerative changes will happen within a specified time frame. While some studies [7,8,10] aimed to predict whether knee OA progresses within a specified duration, others [6,11] tried to predict if a patient will undergo a TKR surgery at some point in the future. However, the common problem of the aforementioned studies is that the scope of knee OA progression is limited to a single period of time or outcome, which substantially differentiates our work from prior art.

Prognosis prediction from imaging data Jung *et al.* [12] proposed a long-short-term-memory (LSTM)-based architecture that performed many-to-many predictions for the prognosis of an Alzheimer’s disease (AD). However, they utilized parameters measured from MR images (e.g. volume), instead of the raw MRI data. Zhang *et al.* [13] studied the same disease but aimed to predict the AD

stage at the next follow-up given the previous MR images. In contrast to the aforementioned methods, we formulate the prognosis prediction problem as a one-to-many model, in which we predict the course of a disease given its initial imaging and clinical data.

Transformers Although originally developed in the field of natural language processing [14,15], transformer-based architectures have recently been applied also in vision tasks [16,17,18]. The primary characteristic of a transformer is the ability to perform sequential tasks in parallel by introducing learnable positional embedding and leveraging a multi-head self-attention (MSA) mechanism. A great benefit of a transformer is being task agnostic, allowing high model capacity while maintaining reasonable speed of computations. In the context of this paper, we use the domain agnostic property of a transformer to process sequences of super-pixels of images, as well as multi-modal data.

3 Method

3.1 Conceptual model

We assume a clinical setting in which multiple decision makers interact to obtain a prognosis for a patient. An example of this is the case when a general practitioner makes treatment decisions based on imaging data \mathbf{x}_0 , as well as additional data \mathbf{m}_0 , e.g. symptomatic assessments. In the context of our work, we treat prognosis as temporal *structural* changes observed by imaging.

Consider the following probability distribution:

$$p(y_0, y_1, \dots, y_K | \mathbf{x}_0, \mathbf{m}_0), \quad (1)$$

where $y_t \in \{0, \dots, N_c - 1\}$ denotes disease severity stages at future follow-ups at times $t \in \{1, \dots, K\}$, and N_c denotes the number of classes. When $t = 0$, we indicate the examination conducted at baseline (first examination).

We can assume that $p(y_0 | \mathbf{x}_0, \mathbf{m}_0) = p(y_0 | \mathbf{x}_0)$, as y_0 denotes imaging findings, described by a radiologist, whose task is to provide the description of the image content. We can then rewrite (1) as

$$p(y_0, y_1, \dots, y_K | \mathbf{x}_0, \mathbf{m}_0) \propto p(y_1, \dots, y_K | y_0, \mathbf{x}_0, \mathbf{m}_0) p(y_0 | \mathbf{x}_0), \quad (2)$$

In the sequel, we represent $p(y_0 | \mathbf{x}_0)$ by a neural network, which predicts the current stage of the disease. $p(y_1, \dots, y_K | y_0, \mathbf{x}_0, \mathbf{m}_0)$ is represented by a second neural network, which leverages the predicted y_0 , image features \mathbf{x}_0 , and the auxiliary patient data \mathbf{m}_0 . The concept is graphically illustrated in Figure 2.

3.2 Transformers for multi-agent decision making

Transformers background Let $\{\mathbf{s}\}_{i=1}^N, \mathbf{s}_i \in \mathbb{R}^{1 \times C}$ denote a sequence of vectors to be encoded by a transformer. Each transformer encoder is a stack of L

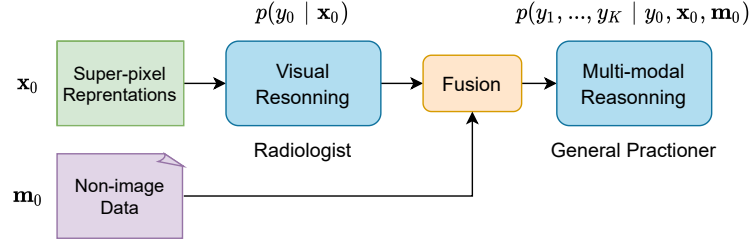


Fig. 2. The conceptual model of the DeepProg framework.

alternating multi-head attention modules, defined as

$$h_0 = [E_{[CLS]}, \mathbf{s}_1, \dots, \mathbf{s}_N] + E_{[POS]}, \quad (3)$$

$$z_{l-1} = \text{MSA}(\text{LN}(h_{l-1})) + h_{l-1}, \quad (4)$$

$$h_l = \text{MLP}(\text{LN}(z_{l-1})) + z_{l-1}, \quad l = \{1, \dots, L\} \quad (5)$$

where $E_{[CLS]} \in \mathbb{R}^{1 \times D}$ is learnable token, indicating a start of $\{\mathbf{s}_i\}_{i=1}^N$, $E_{[POS]} \in \mathbb{R}^{(N+1) \times D}$ is a positional embedding, which is also learnable. MLP is a multi-layer perceptron (i.e. a fully-connected network), LN is the layer normalization [19], and $\text{MSA}(\cdot)$ is a multi-head self-attention layer. A detailed explanation of each of these blocks is given in [14].

Image classification as visual reasoning Figure 3 shows a graphical illustration of the proposed method. Specifically, we first use a CNN to obtain image representations (feature maps), which correspond to the image super-pixels of size $H \times W$. In our notation, C indicates the channel dimension of the feature maps. Having in mind the idea of visual reasoning, we treat representations of size $1 \times 1 \times D$ as the elements of a sequence of size $N = H \times W$, and pass them through a transformer, which predicts $p(y_0 | \mathbf{x}_0)$. As we convert the image classification problem into a sequence classification one, we add two common ingredients: a sequence start vector, denoted by $[CLS]$, and also the positional embeddings for every super-pixel [14,16]. Both of these are learnable vectors, and positional embeddings are added to the superpixels of an image as shown in Figure 3. Once the input sequence of superpixels is passed through the diagnosis transformer D , we take its first element and pass it through a fully connected network, similar to [16].

Multi-modal fusion for prognosis prediction To fuse the predicted \hat{y}_0 and other optional clinical data for predicting the prognosis, we first present each of them as an embedding vector, and then concatenate these vectors into a single embedding representation. We learn the interaction among those multiple modalities by a context network, comprising a fully connected layer, a ReLU activation, and a layer normalization [19].

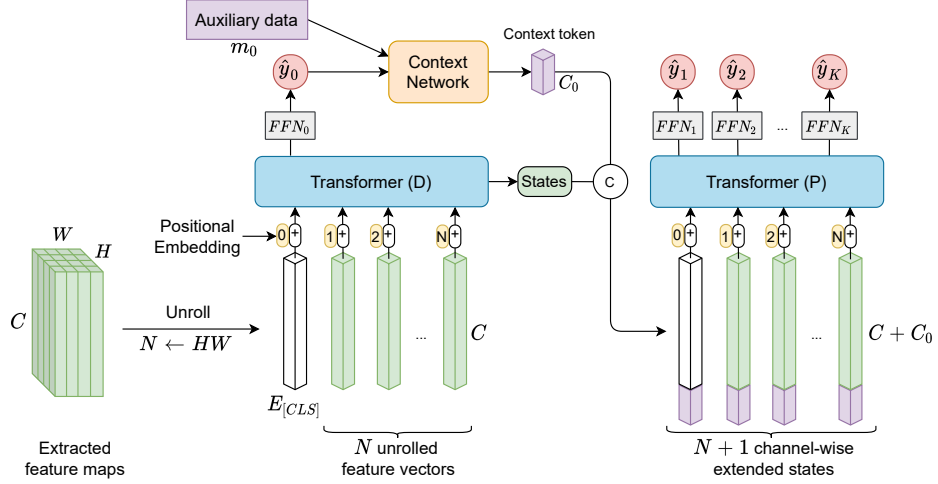


Fig. 3. The workflow of DeepProg.

Once we have obtained a context token with the length C_0 from the context network, we replicate it $N + 1$ times and append them into the output states of the transformer D to form a sequence of vectors having length of $(C + C_0)$ to be used as the input for the prognosis transformer P. To this end, we take the first K elements of the transformer's last layers' outputs, and pass them through K separate feed-forward networks (FFNs), consisting of a layer normalization followed by two fully connected layers separated by a GELU activation [20], to predict the course of a disease.

4 Experiments

4.1 Datasets

Synthetic data We generated a synthetic dataset for the prognosis task from the ChestMNIST dataset [9]. Specifically, we simulated an artificial disease with 9 stages by rotations of aligned chest X-ray images ($m \frac{\pi}{4}$ rad with $m = 0, \dots, 8$). In the experiment, DeepProg takes an image rotated by an unknown angle as input, and predicts that angle, together with rotation angles in the next 4 follow-ups. In the experiment, we tested various transition rates to simulate either a stochastic or deterministic process (probability of 75%, 90%, or 100%).

Osteoarthritis prognosis We conducted experiments on the Osteoarthritis Initiative (OAI), which is publicly available at <https://nda.nih.gov/oai/>. 4,796 participants from 45 to 79 years old participated in the OAI cohort, which consisted of a baseline, and follow-up visits after 12, 18, 24, 30, 36, 48, 60, 72, 84, 96, 108, 120, and 132 months. Bilateral fixed flexion radiographs were imaged

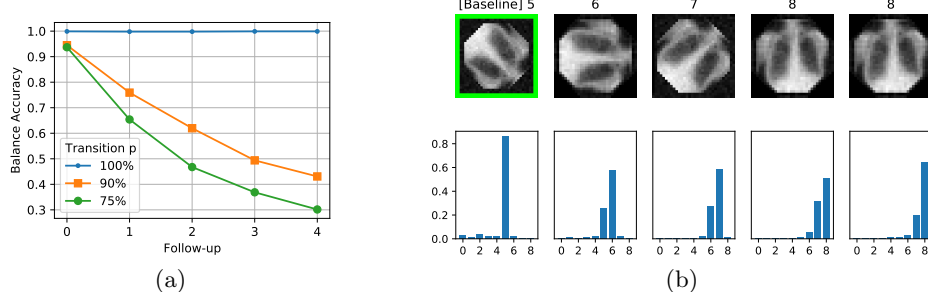


Fig. 4. Diagnosis and prognosis on the synthetic data based on the ChestMNIST dataset. (a) A graphical illustration of DeepProg’s performance depending on the transition probability. (b) The first image in the first row (green boundary) is the input image. The other four images are unobserved by DeepProg, and demonstrate the actual sequence in the data. The bottom row shows the predicted softmax probabilities.

at most of the visits as presented in Suppl. Table S1. In this study, we used all knee images that (i) were annotated for KL grade, (ii) did not include implants, and (iii) were acquired with large imaging cohorts: the baseline, and the 12, 24, 36, 72, and 96-month follow-ups.

The OAI dataset includes data from five acquisition centers, which allowed us to utilize the one-center-out cross-validation procedure: data from 4 centers were used for training and validation, and data from the left-out one for testing. During the training, we also sampled knee images from follow-up examinations to increase the amount of training data. For testing, we evaluated at 6 major time points: the baseline, and 1, 2, 3, 6, and 8 years in the future. For each training set from a group of 4 centers, we performed a 3-fold cross-validation strategy.

Following [7,5,4], we utilized the BoneFinder tool [21] to extract two knees regions of interest from each bilateral radiograph and pre-process each of them. Subsequently, each pre-processed knee image was resized to 256×256 . Since knees that have undergone TKR surgeries at baseline are irrelevant in clinical diagnosis, we excluded them from the dataset.

We utilized the Kellgren-Lawrence (KL) grading system (see Suppl. Figure S1), to assess the knee OA severity. In our experiments, we grouped KL-0 and KL-1 into one class as they are clinically similar, and added TKR knees as the fifth class.

4.2 Implementation details

We trained and evaluated our method and the reference approaches using V100 NVidia GPUs. We implemented all the methods using the Pytorch library [22], and trained each of them with the same set of configurations and hyperparameters presented in Suppl. Tables S2 and S3. To assess the quality of OA prognosis

predictions, we utilized multi-class balanced accuracy (BA) and mean square error (MSE). Additionally, we quantified the OA progression task using F1-score, BA, area under the receiver operating characteristic curve (ROC-AUC), and average precision (AP).

4.3 Synthetic data results

In Figure 4, we demonstrate the performance and the behavior of our method on the synthetic prognosis dataset. Our method perfectly predicts the synthetic prognosis in the deterministic scenario (blue in Figure 4.a) and its performance decays proportionally to the transition probability (orange and green). Additionally, we observe that the method learns that the disease’s stages are ordinal. In Figure 4.b, once the predicted stage reaches the highest level, the model accumulates more confidence for the last stage in the next follow-ups.

4.4 Structural prognosis of osteoarthritis

Knee OA prognosis prediction To our knowledge, this paper is the first in the realm of knee OA prognosis prediction, and thus lacks previous studies to be compared against. As our main reference method, we used the Gaussian state space model (GSSM)-based approach [23], as it naturally enables one-to-many prediction. The results in Figure 5 and Suppl. Table S4 show that DeepProg performed substantially better than GSSM in our setting. Moreover, the figure shows that the inclusion of clinical data helped to improve DeepProg significantly.

Importance of transformer To highlight the role of the transformers in our framework, we conducted an ablation study in which we compared performances of DeepProg with and without both the diagnostic and prognosis transformers. In the baseline setting, we replaced the two transformers by fully-connected layers. On the OAI out-of-site test sets, the involvement of the transformer elements

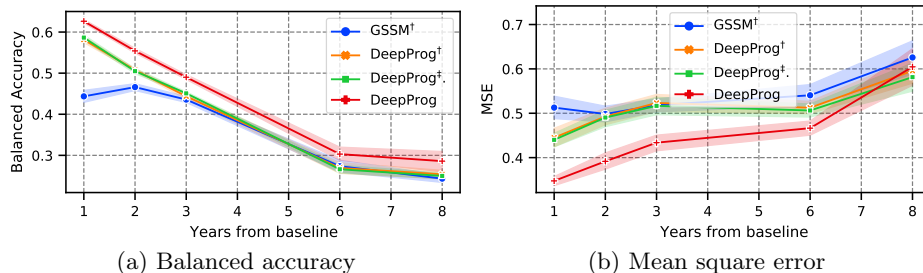


Fig. 5. OA prognosis prediction performances on OAI out-of-site test sets. \dagger and \ddagger indicate the exclusion of clinical data and the transformers from DeepProg, respectively.

Table 1. Comparison with the SOTA approach on the knee OA progression task at the 8 year mark on the OAI out-of-site test set.

Method	BA	F1	ROC-AUC	AP
Tiulpin <i>et al</i> [7]	63.9±1.3	65.0±0.5	68.7±1.2	73.6±1.5
DeepProg	66.2±0.9	64.2±0.8	71.2±1.4	78.2±0.9

significantly improved DeepProg’s prognosis prediction quality throughout the 8 year course (red and green lines in Figure 5).

Knee OA progression prediction Our framework can be integrated with the progression prediction task effortlessly. Instead of using a CNN-based model to predict whether knee OA severity of a knee progresses *within* 8 years from the baseline as [7], our approach enables the simultaneous prediction of knee OA progression within t years, where $t \in \{1, \dots, 8\}$, which was trained alongside the prognosis task. In our experiments, DeepProg significantly outperforms the baseline on multiple metrics as shown in Table 1.

5 Conclusions

In this paper, we proposed a novel general-purpose transformer-based method to predict knee osteoarthritis progression from multi-modal data. To our knowledge, this is the first study in the realm of OA, and the develop method can be of interest to other fields, where a forecasting of disease course is of interest.

Our framework provides tools to integrate multi-modal data beyond one follow-up, and furthermore, has in-built interpretation capabilities (Suppl. Figure S2) through self-attention mechanism. We thus suggest the future studies to investigate these aspects.

Acknowledgments

The OAI is a public-private partnership comprised of five contracts (N01- AR-2-2258; N01-AR-2-2259; N01-AR-2- 2260; N01-AR-2-2261; N01-AR-2-2262) funded by the National Institutes of Health, a branch of the Department of Health and Human Services, and conducted by the OAI Study Investigators. Private funding partners include Merck Research Laboratories; Novartis Pharmaceuticals Corporation, GlaxoSmithKline; and Pfizer, Inc. Private sector funding for the OAI is managed by the Foundation for the National Institutes of Health.

We would like to acknowledge the strategic funding of the University of Oulu, Sigrid Juselius Foundation, Finland.

Dr. Claudia Lindner is acknowledged for providing BoneFinder. Phuoc Dat Nguyen is acknowledged for discussions about transformer.

References

1. S. Glyn-Jones, A. Palmer, R. Agricola, A. Price, T. Vincent, H. Weinans, and A. Carr, “Osteoarthritis,” *The Lancet*, vol. 386, no. 9991, pp. 376–387, 2015.
2. B. Heidari, “Knee osteoarthritis prevalence, risk factors, pathogenesis and features: Part i,” *Caspian journal of internal medicine*, vol. 2, no. 2, p. 205, 2011.
3. J. Kellgren and J. Lawrence, “Radiological assessment of osteo-arthrosis,” *Annals of the rheumatic diseases*, vol. 16, no. 4, p. 494, 1957.
4. A. Tiulpin and S. Saarakkala, “Automatic grading of individual knee osteoarthritis features in plain radiographs using deep convolutional neural networks,” *Diagnostics*, vol. 10, no. 11, p. 932, 2020.
5. H. H. Nguyen, S. Saarakkala, M. Blaschko, and A. Tiulpin, “Semixup: In-and out-of-manifold regularization for deep semi-supervised knee osteoarthritis severity grading from plain radiographs.” *IEEE Transactions on Medical Imaging*, vol. 39, no. 12, pp. 4346–4356, 2020.
6. K. Leung, B. Zhang, J. Tan, Y. Shen, K. J. Geras, J. S. Babb, K. Cho, G. Chang, and C. M. Deniz, “Prediction of total knee replacement and diagnosis of osteoarthritis by using deep learning on knee radiographs: data from the osteoarthritis initiative,” *Radiology*, vol. 296, no. 3, pp. 584–593, 2020.
7. A. Tiulpin, S. Klein, S. M. Bierma-Zeinstra, J. Thevenot, E. Rahtu, J. van Meurs, E. H. Oei, and S. Saarakkala, “Multimodal machine learning-based knee osteoarthritis progression prediction from plain radiographs and clinical data,” *Scientific reports*, vol. 9, no. 1, pp. 1–11, 2019.
8. P. Widera, P. M. Welsing, C. Ladel, J. Loughlin, F. P. Lafeber, F. P. Dop, J. Larkin, H. Weinans, A. Mobasher, and J. Bacardit, “Multi-classifier prediction of knee osteoarthritis progression from incomplete imbalanced longitudinal data,” *Scientific Reports*, vol. 10, no. 1, pp. 1–15, 2020.
9. J. Yang, R. Shi, and B. Ni, “Medmnist classification decathlon: A lightweight automl benchmark for medical image analysis,” *arXiv preprint arXiv:2010.14925*, 2020.
10. B. Guan, F. Liu, A. Haj-Mirzaian, S. Demehri, A. Samsonov, T. Neogi, A. Guermazi, and R. Kijowski, “Deep learning risk assessment models for predicting progression of radiographic medial joint space loss over a 48-month follow-up period,” *Osteoarthritis and cartilage*, vol. 28, no. 4, pp. 428–437, 2020.
11. A. A. Tolpadi, J. J. Lee, V. Pedoia, and S. Majumdar, “Deep learning predicts total knee replacement from magnetic resonance images,” *Scientific reports*, vol. 10, no. 1, pp. 1–12, 2020.
12. W. Jung, A. W. Mulyadi, and H.-I. Suk, “Unified modeling of imputation, forecasting, and prediction for ad progression,” in *International Conference on Medical Image Computing and Computer-Assisted Intervention*. Springer, 2019, pp. 168–176.
13. J. Zhang and Y. Wang, “Continually modeling alzheimer’s disease progression via deep multi-order preserving weight consolidation,” in *International Conference on Medical Image Computing and Computer-Assisted Intervention*. Springer, 2019, pp. 850–859.
14. A. Vaswani, N. Shazeer, N. Parmar, J. Uszkoreit, L. Jones, A. N. Gomez, L. Kaiser, and I. Polosukhin, “Attention is all you need,” in *Advances in neural information processing systems*, 2017, pp. 5998–6008.
15. J. Devlin, M.-W. Chang, K. Lee, and K. Toutanova, “Bert: Pre-training of deep bidirectional transformers for language understanding,” *arXiv preprint arXiv:1810.04805*, 2018.

16. A. Dosovitskiy, L. Beyer, A. Kolesnikov, D. Weissenborn, X. Zhai, T. Unterthiner, M. Dehghani, M. Minderer, G. Heigold, S. Gelly *et al.*, “An image is worth 16x16 words: Transformers for image recognition at scale,” *arXiv preprint arXiv:2010.11929*, vol. 1, 2020.
17. N. Parmar, A. Vaswani, J. Uszkoreit, L. Kaiser, N. Shazeer, A. Ku, and D. Tran, “Image transformer,” in *International Conference on Machine Learning*. PMLR, 2018, pp. 4055–4064.
18. R. Girdhar, J. Carreira, C. Doersch, and A. Zisserman, “Video action transformer network,” in *Proceedings of the IEEE/CVF Conference on Computer Vision and Pattern Recognition*, 2019, pp. 244–253.
19. J. L. Ba, J. R. Kiros, and G. E. Hinton, “Layer normalization,” *arXiv preprint arXiv:1607.06450*, 2016.
20. D. Hendrycks and K. Gimpel, “Gaussian error linear units (GELUs),” 2020, arXiv:1606.08415.
21. C. Lindner, S. Thiagarajah, J. M. Wilkinson, G. A. Wallis, T. F. Cootes, arcOGEN Consortium *et al.*, “Fully automatic segmentation of the proximal femur using random forest regression voting,” *IEEE transactions on medical imaging*, vol. 32, no. 8, pp. 1462–1472, 2013.
22. A. Paszke, S. Gross, F. Massa, A. Lerer, J. Bradbury, G. Chanan, T. Killeen, Z. Lin, N. Gimelshein, L. Antiga *et al.*, “Pytorch: An imperative style, high-performance deep learning library,” *arXiv preprint arXiv:1912.01703*, 2019.
23. R. Krishnan, U. Shalit, and D. Sontag, “Structured inference networks for non-linear state space models,” in *Proceedings of the AAAI Conference on Artificial Intelligence*, vol. 31, no. 1, 2017.
24. D. P. Kingma and J. Ba, “Adam: A method for stochastic optimization,” *arXiv preprint arXiv:1412.6980*, 2014.
25. K. He, X. Zhang, S. Ren, and J. Sun, “Deep residual learning for image recognition,” in *Proceedings of the IEEE conference on computer vision and pattern recognition*, 2016, pp. 770–778.

Supplementary materials



Fig. S1. The Kellgren-Lawrence (KL) system is commonly used to assess the severity of OA. As such, the system classifies OA into 5 grades, which correspond to: no sign of OA, doubtful OA, early OA, moderate OA, and severe OA, respectively.

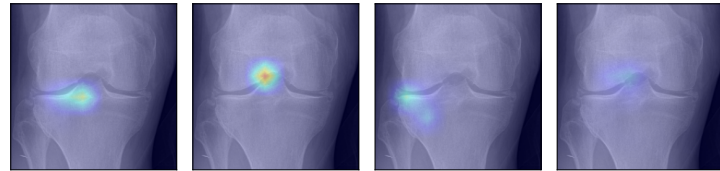


Fig. S2. Example of MSA maps extracted from the prognosis transformer's last layer for a knee with KL 1 at baseline. The attention heads simultaneously focus on different positions along the joint space.

Table S1. OAI dataset description

Visit	KL 0	KL 1	KL 2	KL 3	KL 4	TKR
Baseline	3448	1597	2374	1239	295	61
12 months	3113	1445	2221	1230	355	76
24 months	2893	1348	2079	1172	367	97
36 months	2735	1252	1986	1147	377	135
72 months	1866	1007	471	201	26	9
96 months	1899	987	488	239	47	15

Table S2. Ordered list of augmentations in training

Aug.	Prob.	Parameter
Center cropping	1	700 × 700
Resize	1	280 × 280
Gaussian noise	0.5	0.3
Rotation	1	[-10, 10]
Random cropping	1	256 × 256
Gamma correction	0.5	[0.5, 1.5]

Table S3. Our common hyperparameters

Key	Value
Optimizer	Adam [24]
Beta	[0.95, 0.999]
Learning rate	1e-4
Weight decay	1e-4
Feature extractor	ResNet18 [25]
MSA heads	4
Depth of transformer D	2
Depth of transformer D	8
FFN's bandwidth	256
Dropout rate	0.3

Table S4. Knee OA prognosis prediction performances on the OAI out-of-site test sets. \dagger and \ddagger indicate the exclusion of clinical data and the transformers, respectively.

Year	Method	BA	MSE
1	GSSM \dagger	44.4 \pm 0.9	0.513 \pm 0.016
	DeepProg \dagger	58.2 \pm 0.4	0.445 \pm 0.013
	DeepProg \ddagger	58.6 \pm 0.4	0.440 \pm 0.010
	DeepProg	62.6 \pm 0.3	0.348 \pm 0.006
2	GSSM \dagger	46.6 \pm 0.5	0.498 \pm 0.010
	DeepProg \dagger	50.8 \pm 0.2	0.493 \pm 0.012
	DeepProg \ddagger	50.5 \pm 0.4	0.490 \pm 0.012
	DeepProg	55.4 \pm 0.4	0.392 \pm 0.011
3	GSSM \dagger	43.6 \pm 0.5	0.518 \pm 0.010
	DeepProg \dagger	44.4 \pm 0.4	0.523 \pm 0.013
	DeepProg \ddagger	45.1 \pm 0.2	0.517 \pm 0.013
	DeepProg	49.0 \pm 0.4	0.434 \pm 0.012
6	GSSM \dagger	27.4 \pm 0.8	0.541 \pm 0.015
	DeepProg \dagger	26.9 \pm 0.8	0.512 \pm 0.009
	DeepProg \ddagger	26.6 \pm 0.6	0.506 \pm 0.010
	DeepProg	30.3 \pm 1.0	0.466 \pm 0.011
8	GSSM \dagger	24.3 \pm 0.6	0.626 \pm 0.022
	DeepProg \dagger	25.4 \pm 0.7	0.596 \pm 0.018
	DeepProg \ddagger	25.0 \pm 0.5	0.581 \pm 0.021
	DeepProg	28.6 \pm 1.6	0.605 \pm 0.026